THE JOURNAL OF PHYSICAL CHEMISTRY A

pubs.acs.org/JPCA Article

Structure of Proton-Bound Methionine and Tryptophan Dimers in the Gas Phase Investigated with IRMPD Spectroscopy and Quantum Chemical Calculations

Åke Andersson, Mathias Poline, Meena Kodambattil, Oleksii Rebrov, Estelle Loire, Philippe Maître, and Vitali Zhaunerchyk*

Cite This: *J. Phys. Chem. A* 2020, 124, 2408−2415 Read Online

ACCESS | Metrics & More | Article Recommendations | Supporting Information

ABSTRACT: The structures of three proton-bound dimers (Met_2H^+, $MetTrpH^+$, and Trp_2H^+) are investigated in the gas phase with infrared multiple photon disassociation (IRMPD) spectroscopy in combination with quantum chemical calculations. Their IRMPD spectra in the range of 600−1850 cm^{-1} are obtained experimentally using an FT-ICR mass spectrometer and the CLIO free electron laser as an IR light source. The most abundant conformers are elucidated by comparing the IRMPD spectra with harmonic frequencies obtained at the B3LYP-GD3BJ/6-311++G** level of theory. Discrepancies between the experimental and theoretical data in the region of 1500−1700 cm^{-1} are attributed to the anharmonicity of the amino bending modes. We confirm the result of a previous IRMPD study that the structure of gas-phase Trp_2H^+ is charge-solvated but find that there are more stable structures than originally reported (Feng, R.; Yin, H.; Kong, X. *Rapid Commun. Mass Spectrom.* **2016**, *30*, 24−28). In addition, gas-phase Met_2H^+ and $MetTrpH^+$ have been revealed to have charge-solvated structures. For all three dimers, the most stable conformer is found to be of type A. The spectrum of Met_2H^+, however, cannot be explained without some abundance of type B charge-solvated conformers as well as salt-bridged structures.

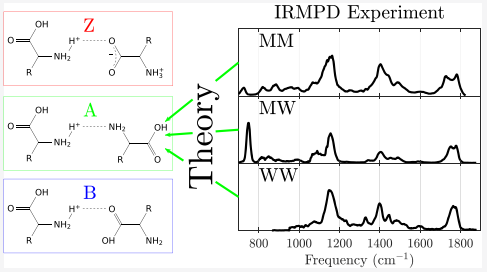

INTRODUCTION

Amino acids are ubiquitous building blocks for life. They consist of an amino group, a carboxyl group, and a side chain which determines the properties of the specific amino acid. In solution, interactions with the solvent molecules cause amino acids to take on a zwitterionic form, meaning that a proton has moved from the carboxyl to the amino functional group. In the context of gas-phase studies of isolated and microsolvated amino acids, the question of when and how amino acids become zwitterions has been studied widely.[1−29] In many of these studies, infrared multiple photon disassociation (IRMPD) spectroscopy has been used as an experimental tool for molecular structure elucidation.

Protonated α-amino acid dimers in the gas phase are of interest because they capture the essence of amino acid interaction while being of a relatively small size. They exhibit many conformers, commonly classified as charge-solvated (CS) or salt-bridge (SB) structures. The CS implies the binding of the monomers through an intermolecular hydrogen bond (H-bond) between the protonated amino group of one amino acid and the amino group (type A) or carboxyl group (type B) of another amino acid. In the SB structures, one monomer adopts a zwitterionic (type Z) form.

The stability of SB structures is related to the stability of a monomer's zwitterionic form, which in turn has been attributed to various factors. Wyttenbach et al.[2] found a positive correlation between the stability of the zwitterionic form of alkali metal-cationized amino acid monomers and the proton affinity (PA) of the amino acid. Bush et al.[3] found this correlation to be weaker for alkali metal-cationized lysine with additional methyl groups and argued that PA is not a reliable indication of zwitterionic stability whereas side chain effects are more important. By contrast, studies of proton-bound amino acid homodimers have shown that the zwitterionic stability is well predicted by PA.[4−11] High PA amino acids, e.g., arginine, lysine, and proline, have been shown to form SB dimers.[4−6] On the other hand, low PA amino acids, e.g., glycine, threonine, phenylalanine, and tyrosine, form CS dimers.[7−10] With a mid-PA, glutamic acid has been shown to adopt CS structures at 15 K but SB dimer structure at 300 K.[11] A recent study by Feng et al.[1] of tryptophan dimers has shown it to favor CS over SB, even though its PA is similar to that of proline.

In this article, we report the results of IRMPD studies performed for Met_2H^+, $MetTrpH^+$, and Trp_2H^+ in the

Received: December 21, 2019
Revised: February 22, 2020
Published: February 27, 2020

https://dx.doi.org/10.1021/acs.jpca.9b11811
J. Phys. Chem. A 2020, 124, 2408−2415

frequency range of 600−1850 cm^{-1}. The tryptophan (Trp, W) homodimer is studied with the aim of revealing its IRMPD spectrum in a previously unexplored frequency range.[1] Studies of the methionine (Met, M) homodimer are motivated by the fact that its PA lies in the frontier of amino acids that are known to form CS structures.[10,30] An additional reason to study Met is its side chain. Dimers of amino acids tend to stabilize their geometry through intermolecular interaction, e.g., H-bonding between side chains, in addition to the CS or SB binding. Methionine has no N, O, or F on its side chain, only S, which forms significantly weaker H-bonds.[31,32] It is therefore of interest to study how methionine dimers stabilize. It is also of interest to study Met heterodimers, where the second monomer is prone to intermolecular interactions. For this purpose, the $MetTrpH^+$ dimer is studied, which has only the Trp side chain capable of significant intermolecular interaction, presumably N−H···N and N−H···π to the indole ring.

METHODS

Experiment. All experimental data was collected at Centre Laser Infrarouge d'Orsay (CLIO) in Orsay, France. Three amino acid dimers were studied: Met_2H^+, $MetTrpH^+$, and Trp_2H^+. The Trp used for Trp_2H^+ was an isotopologue; specifically, five deuterium atoms were substituted on the indole ring. The dimer solutions were prepared as a 1 mM monomer concentration in a 49:49:2 mixture of water, methanol, and formic acid. Ions were delivered to the gas phase by electrospray ionization (ESI) of the solution and subsequently stored and accumulated in a linear ion trap of a mass spectrometer (MS) of model 7 T Bruker Apex Qe. While trapped, ions were subsequently pulse extracted toward the ion cyclotron resonance (ICR) ion trap, where they were irradiated with pulses of the CLIO free electron laser (FEL), which scanned the 600−1850 cm^{-1} frequency range. The FEL beam had a power of 20−30 mW and a pulse rate 25 Hz. The irradiation time of the ions was controlled by a mechanical shutter placed between the FEL beam and the ICR ion trap. It is typically chosen to be around 500 ms. The measurements were performed at high, mid, and low irradiation energies, meaning that the summed energy of the FEL pulses over the irradiation time was above, in, and below the range of 8−16 mJ, respectively. Finally, the abundance of dimers and their fragments were analyzed using Fourier transform ICR (FT-ICR) in the MS.

For a given FEL frequency, the IRMPD intensity was calculated as

$$I_{\mathrm{IRMPD}} = \ln\left(1 + \frac{I_{\mathrm{fragment}}}{I_{\mathrm{parent}}}\right)$$

where $I_{\langle \mathrm{species} \rangle}$ is the integrated MS intensity of that species and its isotopologues. Dimers Met_2H^+, $MetTrpH^+$, and Trp_2H^+ fragment into $MetH^+$, $TrpH^+$, and $TrpH^+$, respectively. Under high irradiation, these may fragment further. In that case, I_{fragment} is replaced by the sum of all of the fragments' intensities.

Calculations. A conformational search was performed using several molecular dynamics (MD) simulations with different initial geometries in order to cover a large conformation space. The MD calculations were carried out in the microcanonical ensemble employing the density functional-based tight binding method[33] as implemented in the DFTB+ software package.[34] The initial velocities were considered to correspond to a Maxwell−Boltzmann distribution at 298 K, and a velocity Verlet algorithm with a time step of 1 fs was implemented. For amino acid heterodimer $MetTrpH^+$, we considered two sets of structures with either the Met or Trp moiety being protonated.

The most stable structures obtained with the MD simulations were optimized with DFT using the B3LYP functional and the 6-311++G** basis set including the GD3BJ empirical dispersion. Harmonic frequency analysis was performed at the same level of theory. For the optimized structures, single-point energies were calculated with the CBS-4M composite method. To obtain the corresponding Gibbs energies, the CBS-4M calculations were combined with vibrational analyses performed with the B3LYP-GD3BJ/6-311++G** method. For Met_2H^+ dimers, we additionally performed VPT2 anharmonic vibrational analysis as well as single-point energy calculations at the G4MP2 level of theory. To reduce computational costs, the VPT2 analysis was performed with the N07D basis set, which has been shown to perform well under similar circumstances.[35] We note that for $MetTrpH^+$ and Trp_2H^+ dimers, which have more complex structures, neither G4MP2 calculations nor the VPT2 analysis was undertaken due to limitations in computational time. All of these calculations were carried out with the Gaussian 16 program.[36]

When comparing the harmonic frequency analysis of conformers with an experimental spectrum, three modifications are made. First, all frequencies are multiplied by 0.980 to account for anharmonicity. This frequency scaling constant was found by least-squares fitting of harmonic theory to all experimental spectra and is consistent with B3LYP frequency scaling for other molecules.[37] Second, for every conformer, its vibrational frequencies are broadened into a continuous spectrum by convolution with a Gaussian function with parameter σ = 8 cm^{-1} or equivalently with a full width at half-maximum of 18.8 cm^{-1}. This broadening was required in order to take into account the FEL pulse line width. Finally, the spectra of conformers are scaled in proportion to their relative abundances at room temperature and summed. The relative abundances p_i were found to be

$$p_i = \frac{1}{Z}\exp\left(-\frac{G_i}{k_{\mathrm{B}}T}\right);\ Z = \sum_i \exp\left(-\frac{G_i}{k_{\mathrm{B}}T}\right) \quad (1)$$

where G_i represents the Gibbs energies of the conformers, k_B = 8.314 J $mol^{-1}K^{-1}$ is the Boltzmann constant, and T is the temperature.

With the goal of understanding and classifying the intermolecular and weak intramolecular interactions, noncovalent interaction (NCI) analyses were performed for the most abundant conformers of Met_2H^+, $MetTrpH^+$, and Trp_2H^+. The NCI method introduced by Johnson et al.[38] uses the electron density ρ, its gradient, and the second largest eigen value λ_2 of its Hessian, to classify real-space regions as van der Waals interactions, H-bonds, or steric repulsions. The sign(λ_2)ρ index assigned by the NCI method can also be related to the binding energy of H-bonds.[39]

RESULTS AND DISCUSSION

Methionine−Methionine Dimers. The four most abundant structures of Met_2H^+ at T = 300 K are shown in Figure 1a. As inferred from our NCI analyses (Figure S4 in SI), in all

https://dx.doi.org/10.1021/acs.jpca.9b11811
J. Phys. Chem. A 2020, 124, 2408−2415

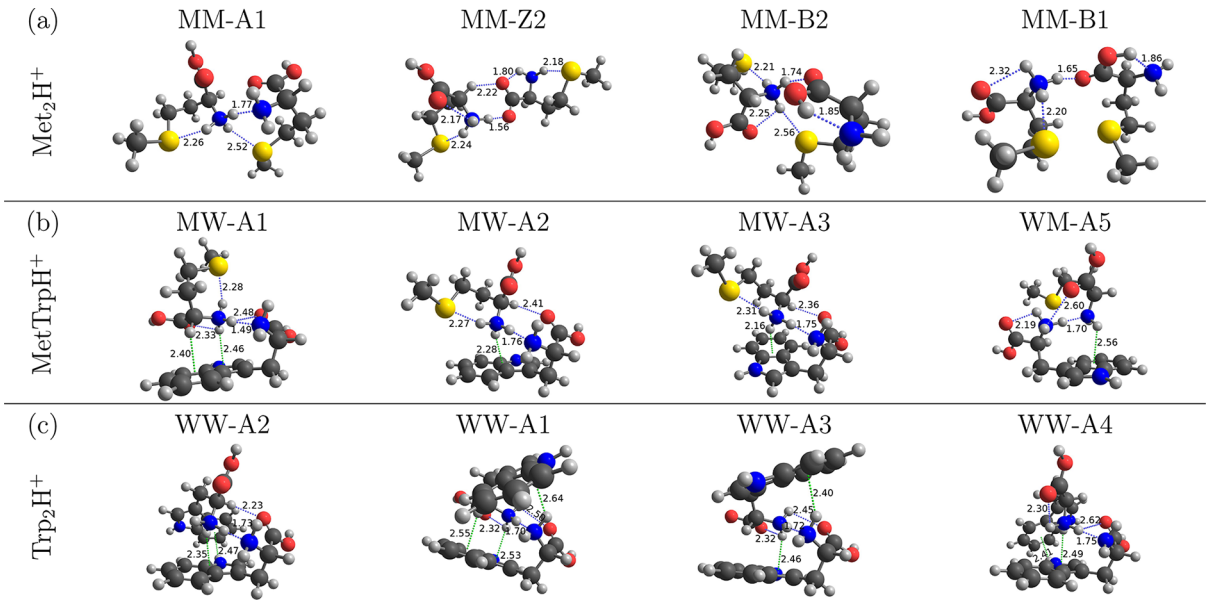

Figure 1. Conformers of (a) Met_2H^+, (b) $MetTrpH^+$, and (c) Trp_2H^+ with the lowest Gibbs energies at T = 300 K. The distances in angstroms of possible H-bonds (blue dotted lines) and cation−π interactions (dotted green lines) are shown. The strength of these interactions is investigated in our NCI analysis (Figures S4−S6 in the SI). The shorthand XY-SN denotes a dimer structure. X and Y are one-letter amino acid codes of the protonated and unprotonated moieties, respectively. S is the structure type, which can be A, B, or Z. N is the index when sorted among structures of the same type, with respect to electronic energy at the CBS-4M level of theory.

four, the S on the protonated moiety forms an intramolecular H-bond with the protonated amino group, causing the side chain to bend. In MM-A1 and MM-B2, the other S weakly interacts with the protonated amino group, stabilizing the dimer further. In MM-B1, MM-B2, and MM-Z2, an H-bond is formed between the amino and carboxyl groups of the unprotonated moiety.

The single-point energies of Met_2H^+ were calculated at three levels of theory. In order of increasing accuracy and computational expense, they are B3LYP, CBS-4M, and G4MP2. An energy comparison of the methods is made in Figure 2. Compared to the composite methods (CBS-4M and

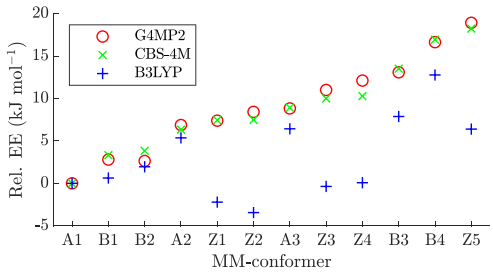

Figure 2. Electronic energy for Met_2H^+ conformers relative to MM-A1, calculated at three levels of theory. The geometries of all Met_2H^+ conformers are available as Supporting Information (Figure S1 in the SI).

G4MP2), B3LYP greatly underestimates the energy of SB conformers. A similar tendency was previously reported in studies of serine dimers.[20] The CBS-4M electronic energy calculations of Met_2H^+ conformers give results consistent with G4MP2 while having the advantage of being less time-consuming. In light of this agreement, CBS-4M is assumed to be suitable for energy calculations for the two other proton-bound dimers studied in this article. The Gibbs energies of Met_2H^+ conformers were therefore calculated with CBS-4M, and the corresponding relative abundances are shown in Figure 3a.

The IRMPD spectra of Met_2H^+ with different irradiation energies are shown in Figure 4, together with harmonic frequency analyses for the four most abundant conformers. The Gibbs energy analysis based on eq 1 predicts the MM-A1 conformer to be the most abundant species, though its relative population constitutes less than 40%. This is consistent with the experimental data; by comparing the IRMPD spectrum near 1405 cm^{-1} and 1725 cm^{-1} to the harmonic frequency analyses, MM-A1 can be ruled out to be the only populated conformer. Predictions for MM-Z2 lack the second peak in 1700−1800 cm^{-1} region of the experimental spectrum and, therefore, it can also be ruled one as the only populated conformer. The peaks in this region are associated with carboxyl group stretching and, since the type-Z conformer possesses one carboxyl group, it exhibits one peak. The observed peak at 1725 cm^{-1}, being unmatched by MM-A1 and MM-Z2, leads us to believe that there is a substantial abundance of MM-B2 or MM-B1, which both agree well with the experimental IRMPD spectrum. This is again consistent with the Gibbs energy population analysis, which predicts their relative populations to be 11 and 10%, respectively. All conformers except for MM-B1 are predicted to have large peaks in the region of 1500−1700 cm^{-1}, but the IRMPD intensity in this region is constrastingly low and flat. The frequencies in this region correspond to bending modes of the amino group. Because the amino group participates in the H-bonding of the dimer and the potential along the proton transfer coordinate is quite flat, we believe these modes to be strongly anharmonic and harmonic analyses to be insufficient. This anharmonicity is known to play a significant role in H-bonding amino stretching in Lys_2H^+,[40,41] so it is plausible that bending is also affected.

In order to shed more light on the discrepancies in the region of 1500−1700 cm^{-1}, a VPT2 anharmonic vibrational

https://dx.doi.org/10.1021/acs.jpca.9b11811
J. Phys. Chem. A 2020, 124, 2408−2415

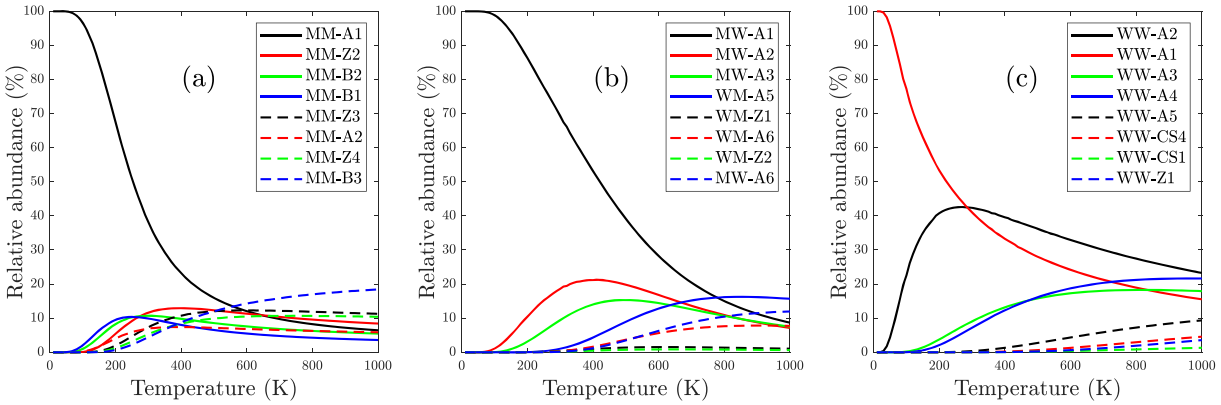

Figure 3. Temperature-dependent relative abundances for the eight most abundant (at 300 K) conformers of (a) Met_2H^+, (b) $MetTrpH^+$, and (c) Trp_2H^+, obtained with eq 1 by employing the CBS-4M method for calculating Gibbs energies. The relative abundances do not sum to exactly 1 because additional conformers were considered when calculating the thermodynamic partition function. Note that because conformers are indexed by type and electronic energies, not by type and Gibbs energies, some low-index conformers, e.g., WM-A1, are not among the eight most abundant conformers.

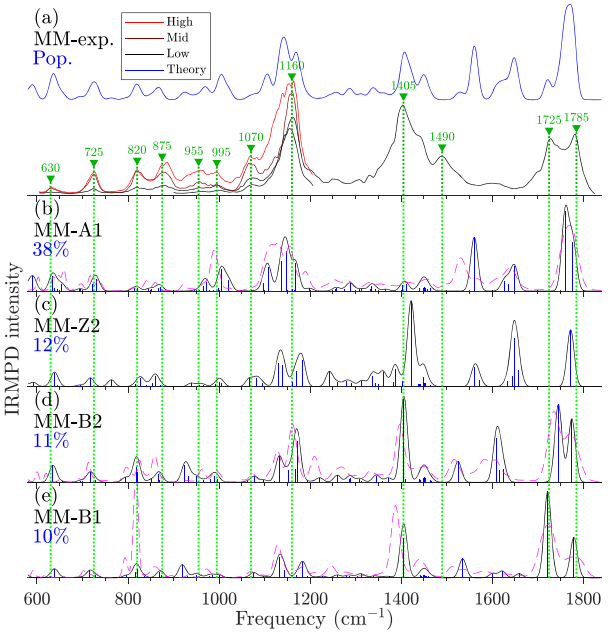

Figure 4. IRMPD spectra of Met_2H^+. (a) The experimental IRMPD spectra measured at different irradiation energies (black/wine/red solid lines), with local maxima highlighted (green triangles) and traced. The sum of predicted spectra of conformers weighted by relative abundances from Figure 3a (blue line) is included for comparison and offset to ease viewing. (b–e) Scaled harmonic frequencies (solid blue lines) of individual conformers and their relative abundance (blue text) obtained from eq 1. Predicted spectra (solid black lines) were obtained by convoluting with a Gaussian function with fwhm = 18.8 cm^{-1}. The anharmonic VPT2 alternative (dashed magenta lines) is included for comparison.

analysis was performed. The resulting spectra are shown as dashed magenta lines in Figure 4. The anharmonic analysis of MM-Z2 did not produce a sensible result. For abundant conformers of types A and B, the anharmonic analyses indeed predict flatter and less intense IRMPD spectra in the region of 1500–1700 cm^{-1}. Furthermore, the VPT2 bands are red-shifted compared to those predicted by the harmonic analysis. Overall, the anharmonic treatment improves agreement with the experiment.

It is interesting that the VPT2 bands of MM-B2 fit the experimental spectra better than those of MM-A1, calling into question whether MM-A1 is truly the most abundant. This can point to the nonthermal population of conformers produced upon ESI. Although this phenomenon was observed in previous studies performed with other experimental setups,[42] this scenario is very unlikely in our case. When the ions accumulate in the linear ion trap of the ICR, multiple low-energy collisions with the Ar buffer gas atoms occur, leading to a thermalization of the ions. On the other hand, a relatively low predicted abundance for the MM-B2 conformer might point to deficiencies of the theoretical calculations.

Methionine–Tryptophan Dimers. The four most abundant structures of $MetTrpH^+$ at T = 300 K are shown in Figure 1b. All structures shown are type A and, according to our NCI analyses (Figure S5 in SI), are additionally stabilized by a cation–π interaction between the amino group of the Met moiety and the indole ring. A weak intermolecular interaction exists between either the amino group (MW-A1, WM-A5) or the α-H (MW-A2, MW-A3) of the protonated moiety and carboxyl group. For the case when the Met moiety is protonated, its side chain bends due to an H-bond between the S and the amino group, similar to the Met_2H^+ case. In MW-A1, there is an additional cation–π interaction between Met α-H and the phenyl part of the indole ring, making MW-A1 the most stable structure by far.

Following the conclusion drawn from the Met_2H^+ results, the electronic energies of $MetTrpH^+$ were calculated with CBS-4M and are shown in Table 1. The Gibbs energies of $MetTrpH^+$ conformers were calculated, and the corresponding relative abundances are shown in Figure 3b. As follows from the figure, the MW-A1 conformer is the most abundant species over a broad temperature range.

The IRMPD spectra of $MetTrpH^+$ for different irradiation energies are shown in Figure 5, together with harmonic frequency analyses for the four most abundant conformers and the most abundant conformers of types B and Z. The experimental IRMPD spectra show that there is a large peak at 750 cm^{-1}, substantially larger than the one at 995 cm^{-1}. According to the harmonic frequency analysis, all conformers are predicted to have a peak near 750 cm^{-1}, but only the three most abundant conformers are predicted to have a peak near 995 cm^{-1}, though of magnitude similar to that of the 750 cm^{-1}

https://dx.doi.org/10.1021/acs.jpca.9b11811
J. Phys. Chem. A 2020, 124, 2408–2415

Table 1. Relative Electronic Energies (EE) of the Most Stable MetTrpH$^+$ and Labeled Trp$_2$H$^+$ Conformers, Calculated with CBS-4M[a]

conf.	EE (kJ mol^{-1})	conf.	EE (kJ mol^{-1})
MW-A1	0.00	WW-A1	0.00
MW-A2	4.67	WW-A2	1.14
MW-A3	7.06	WW-A3	5.87
WM-A1	10.55	WW-A4	6.89
WM-Z1	14.98	WW-A5	15.10
WM-A2	15.76	WW-CS4[b]	21.26
WM-A3	15.77	WW-CS1[b]	21.49
WM-Z2	15.93	WW-A6	29.68
WM-A4	16.44	WW-Z1	31.33
WM-A5	17.41	WW-B1	40.43

[a]The first letter in the dimer notation is the name of the amino acid where the proton is located. The geometries of all MetTrpH$^+$ and Trp$_2$H$^+$ conformers are available as Supporting Information (Figures S2 and S3, respectively). [b]These conformer structures were originally found by Feng et al.[1] and later provided to us upon request. They are both type A, but we use their original name.

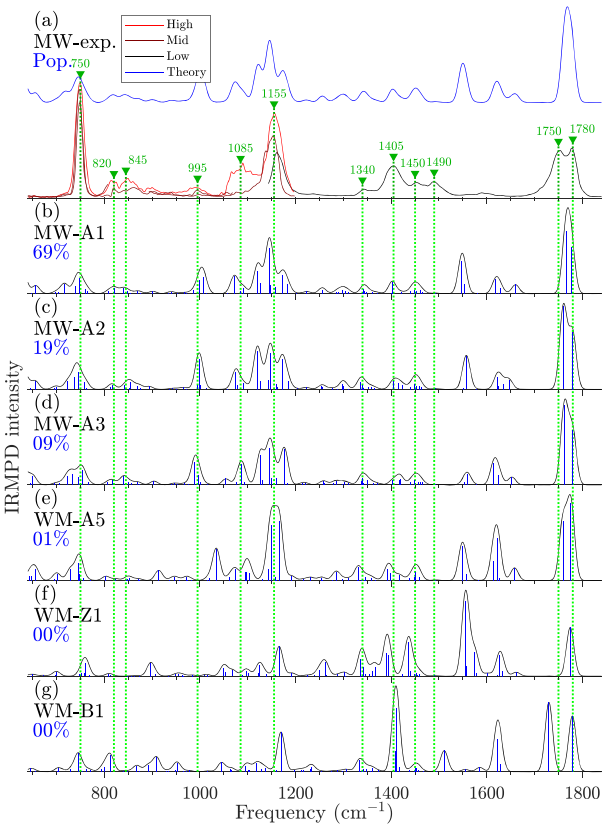

Figure 5. The same as for Figure 4, but for MetTrpH$^+$ and without VPT2. WM-Z1 and WM-B1 are ranked 5 and 16 in abundance, respectively.

peak. The experimental scan with high irradiation energy revealed a peak at 1085 cm^{-1}, which is present only for the conformers of type A. As was the case for Met$_2$H$^+$, the type-Z conformer is predicted to have only a single peak in the region of 1700−1800 cm^{-1}. Therefore, it is unlikely to be significantly populated, which is in line with the population analysis based on eq 1. Again, we observe low and flat IRMPD intensity in the region of 1500−1700 cm^{-1}, but harmonic analyses predict relatively intense peaks there. Anharmonic analyses were not undertaken due to limitations on computational time, but we hypothesize that the peaks in the region of 1500−1700 cm^{-1} would have become less intense, as they did for Met$_2$H$^+$. The harmonic analyses for the three most abundant conformers all fit the experimental spectra adequately, which is consistent with the populations obtained from the Gibbs energies using eq 1.

It is interesting that despite the fact that in the most abundant MetTrpH$^+$ conformers the proton is located on the Met moiety, as seen in Figure 1b, the IRMPD mass spectra of MetTrpH$^+$ do not show MetH$^+$ fragments, only TrpH$^+$. A plausible explanation can be suggested on the basis of the multiphoton nature of the IRMPD process. The successive photon absorption is not instantaneous since it is determined by the intramolecular vibrational energy redistribution time scale. This implies that the dimer can undergo conformational conversion such that the proton might migrate from Met to the Trp moiety. Another explanation for this observation could be that the TrpH$^+$ + Met fragmentation channel is more energetically favorable than MetH$^+$ + Trp. In order to justify this explanation, we calculated the energies of these channels as the difference between the enthalpies at T = 300 K of the corresponding fragments and the parent dimer assuming the lowest-energy conformer, MW-A1. The enthalpies for MetH$^+$, TrpH$^+$, Met, and Trp were found with the CBS-4M method (single-point energy calculation) for which the geometries were optimized at the B3LYP-GD3BJ/6-311++G** level of theory. According to our calculations, the energies of the TrpH$^+$ + Met and MetH$^+$ + Trp channels are 158 and 160 kJ mol^{-1}, respectively. Although the TrpH$^+$ + Met channel is indeed energetically more favorable, it is not likely that the difference of only 200 J mol^{-1} explains the predominance of the TrpH$^+$ + Met fragmentation channel. Therefore, we believe that the absence of the MetH$^+$ fragment in the mass spectra provides evidence for isomerization occurring during the IRMPD process. Isomerization has been observed in the IRMPD process for other ions,[43,44] and thus it is not very surprising that it also occurs for proton-bound dimers, which have almost no barrier to proton transfer.[45]

Tryptophan−Tryptophan Dimers. The four most stable structures of Trp$_2$H$^+$ at T = 300 K are shown in Figure 1c. They are all type A and are additionally stabilized by cation−π as well as intermolecular H interaction, as is inferred from the NCI analyses (Figure S6 in SI). In addition to the characteristic H-bond of the type A structures, every structure has a stabilizing weak interaction between either the amino group (WW-A1, WW-A3, WW-A4) or the α-H (WW-A2) of the protonated moiety and the carboxyl group. WW-A1 is set apart from the rest by having three relatively strong stabilizing cation−π interactions from each amino group to the indole N on the other moiety.

The electronic energies of Trp$_2$H$^+$ were calculated with CBS-4M and are listed in Table 1. Two structures previously reported,[1] WW-CS1 and WW-CS4, are included among those found by our conformational search. The Gibbs energies of Trp$_2$H$^+$ conformers were calculated, and the corresponding relative abundances are shown in Figure 3c. It is interesting that even though WW-A1 is the most stable at low temperatures, WW-A2 becomes slightly more abundant at T = 300 K. Such behavior can be explained in terms of entropy. The many cation−π interactions in WW-A1 constrain the side chains and limit the entropy, while the relative floppiness of WW-A2 allows for a higher entropy. Our calculations show

https://dx.doi.org/10.1021/acs.jpca.9b11811
J. Phys. Chem. A 2020, 124, 2408−2415

that the entropy of WW-A1 is indeed $0.6k_B$ (5 J mol^{-1} K^{-1}) lower than that of WW-A2.

For Trp_2H^+, the seven most abundant conformers are type A. Feng et al.[1] have already asserted that the most abundant conformers of Trp_2H^+ are type A. The most stable conformer found in the current article has electronic energy and Gibbs energy 21.26 and 17.96 kJ mol^{-1} lower than those for WW-CS4, which we find to be the most stable conformer among those previously reported. To rule out the possibility that the discrepancy between the findings of Feng et al. and our findings is caused by using different numerical methods, we also calculated electronic energies at the same level of theory. Employing the M062X functional as used in ref 1, the electronic and Gibbs energies of WW-A1 are still lower, by 22.97 and 20.29 kJ mol^{-1}, respectively, than those of WW-CS1.

The IRMPD spectra of Trp_2H^+ in the region of 950−1850 cm^{-1} for different irradiation energies are shown in Figure 6,

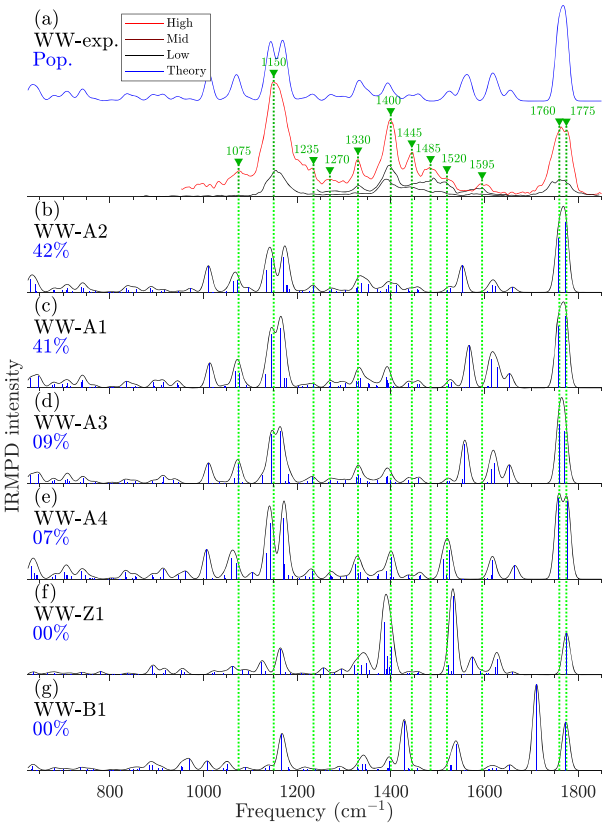

Figure 6. The same as for Figure 4, but for Trp_2H^+ and without VPT2. WW-Z1 and WW-B1 are ranked 8 and 9 in abundance, respectively.

together with harmonic frequency analyses for the four most abundant conformers. Due to issues arising from a contaminant in the MS, IRMPD spectra below 950 cm^{-1} could not be obtained. Similar to the Met_2H^+ and $MetTrpH^+$ cases, there is reasonable agreement between observations and theoretical predictions outside the region of 1500−1700 cm^{-1} for conformers of type A. WW-B1 can be ruled out because of its predicted peak near 1700 cm^{-1} not seen in experimental IRMPD spectra. WW-Z1 has only one peak in the carboxyl region, i.e., 1700−1800 cm^{-1}, while two peaks are actually observed. We thus conclude that the structure of Trp_2H^+ is type A in the gas phase. Because the most stable structures are all type A, their predicted IRMPD spectra are quite similar (Figure 6b−e) and their relative abundances cannot be inferred from the experimental IRMPD spectra unambiguously. Nonetheless, employing abundances based on the Gibbs energy analysis (eq 1), the combined theoretical spectrum (blue line in Figure 6a) agrees reasonably well with the experimental IRMPD spectrum.

CONCLUSIONS

In this article, we investigated the structure of Met_2H^+, $MetTrpH^+$, and Trp_2H^+ dimers. For this purpose, we employed IRMPD spectroscopy in combination with theoretical calculations. On the basis of the comparison of the observed IRMPD spectra with harmonic frequencies of low-energy conformers, scaled by 0.980 to compensate for anharmonicity, it is concluded for all three dimers that the most abundant conformer is CS. For $MetTrpH^+$ and Trp_2H^+, we further conclude that the most abundant conformers are type A, but we cannot differentiate the most stable type A conformers because their predicted spectra were quite similar. In the absence of distinct conformer-specific spectral features, the relative abundances of conformers calculated with eq 1 were used, where Gibbs energies are input parameters. The conformer abundances obtained in such a way provide reasonable agreement of the experimental IRMPD spectra with the combined theoretical IR spectra.

To calculate the Gibbs energy, three methods were used for the B3LYP-GD3BJ/6-311++G** optimized geometries: B3LYP, CBS-4M, and G4MP2. It was found that CBS-4M behaved similarly to G4MP2 for Met_2H^+ while being significantly cheaper and was therefore utilized for all energy calculations. It was also found that B3LYP underestimates the energies of the type-Z conformers.

Trp_2H^+ was studied previously by Feng et al.[1] Our results for Trp_2H^+ confirm that the most stable structure of Trp_2H^+ is type A but includes five more stable structures, of which the most stable has electronic energy and Gibbs energy that are 21.26 and 17.96 kJ mol^{-1} lower than the most stable among those previously reported.

The harmonic frequency analyses adequately describe most of the observed IRMPD features with the exception of those in the region of 1500−1700 cm^{-1}, where the experimental IRMPD features are rather weak and flat. The harmonic analyses assign these peaks to amino bending vibrational modes and overestimate their intensities. We believe these modes to be anharmonic because they involve hydrogen bonds between amino groups, and the potential for proton hopping between the two moieties is rather flat. Anharmonic analyses using VPT2 improves the agreement with the experimental data in the region of 1500−1700 cm^{-1}, with the notable exception of MM-Z2, for which VPT2 does not produce a sensible result.

As mentioned in the Introduction, the aim of this study was to understand how the side chains stabilize. The cation−π interaction is seen for Trp_2H^+ between the indole ring and any sufficiently positive hydrogen, e.g., those adjacent to N and α-H, though the latter is rather uncommon. S···H bonding in Met_2H^+ is concluded to occur between S and protonated amino groups. For the $MetTrpH^+$ heterodimer, side chain stabilization occurs through both. If the Met moiety amino group is protonated, then it interacts with (in order of decreasing NCI index ρ) the Trp amino group, S, and the indole ring. Otherwise, in many structures including the most

https://dx.doi.org/10.1021/acs.jpca.9b11811
J. Phys. Chem. A 2020, 124, 2408−2415

abundant, the protonated Trp amino group interacts only with the Met amino and carboxyl group, and the S does not participate in a significant interaction.

Tryptophan and proline may be remarkable counterexamples to the empirical rule which states that the stability of SB structures of homodimers increases with the PA of the monomer.[8] The uncertainty lies in which of those amino acids have the greatest PA because they are not consistently ranked across works. (See ref 30 and references therein.) The same can be said for methionine and proline. We speculate that while the PA of an amino acid is a mostly reliable indicator for whether the homodimer structure is SB, other properties, e.g., side chains, affect the structure type when the PA is "on the fence". This seems to be the case for amino acids which lie near proline on the PA scale.[10]

In the future, we plan to investigate diastereomer-specific IR features of homo- and heterochiral amino acid dimers. Such studies are essential to developing analytical tools for characterizing the sample enantiomeric purity. The very recent studies on proton-bound glutamic acid dimers have demonstrated the experimental evidence for the chiral recognition of amino acid dimers from their IR spectra.[11] Furthermore, we have recently reported similar studies on different amino acid dimers from theoretical perspectives, which has also verified the potential of this approach.[46] The results presented in this article were obtained for homochiral dimers, and thus they can readily complement our envisioned studies.

■ ASSOCIATED CONTENT

Supporting Information

The Supporting Information is available free of charge at https://pubs.acs.org/doi/10.1021/acs.jpca.9b11811.

Figures S1−S6 referred to in this article and tables of the Cartesian coordinates of each of the 44 conformers (PDF)

■ AUTHOR INFORMATION

Corresponding Author

Vitali Zhaunerchyk − *Department of Physics, University of Gothenburg, 405 30 Gothenburg, Sweden;* orcid.org/0000-0001-7302-7413; Email: vitali.zhaunerchyk@physics.gu.se

Authors

Åke Andersson − *Chalmers University of Technology, 412 96 Gothenburg, Sweden*

Mathias Poline − *Department of Physics, Stockholm University, 114 19 Stockholm, Sweden*

Meena Kodambattil − *Department of Physics, University of Gothenburg, 405 30 Gothenburg, Sweden; International School of Photonics, Cochin University of Science and Technology, Kochi, Kerala 682022, India*

Oleksii Rebrov − *Department of Physics, Stockholm University, 114 19 Stockholm, Sweden*

Estelle Loire − *Laboratoire de Chimie Physique (UMR8000), Université Paris-Sud, CNRS, Université Paris Saclay, Orsay 91405, France*

Philippe Maître − *Laboratoire de Chimie Physique (UMR8000), Université Paris-Sud, CNRS, Université Paris Saclay, Orsay 91405, France;* orcid.org/0000-0003-2924-1054

Complete contact information is available at: https://pubs.acs.org/10.1021/acs.jpca.9b11811

Notes

The authors declare no competing financial interest.

■ ACKNOWLEDGMENTS

We are thankful to the CLIO staff for help and assistance with performing the experiment. M.K. thanks the Erasmus+ EU program for providing her with a scholarship. This project has received funding from the European Union's Horizon 2020 research and innovation programme under grant agreement no. 731077. Calculations were performed with resources at the Chalmers Centre for Computational Science and Engineering (C3SE) provided by the Swedish National Infrastructure for Computing (SNIC).

■ REFERENCES

(1) Feng, R.; Yin, H.; Kong, X. Structure of Protonated Tryptophan Dimer in the Gas Phase Investigated by IRPD Spectroscopy and Theoretical Calculations. *Rapid Commun. Mass Spectrom.* **2016**, *30*, 24−28.

(2) Wyttenbach, T.; Witt, M.; Bowers, M. T. On the Stability of Amino Acid Zwitterions in the Gas Phase: The Influence of Derivatization, Proton Affinity, and Alkali Ion Addition. *J. Am. Chem. Soc.* **2000**, *122*, 3458−3464.

(3) Bush, M. F.; Oomens, J.; Williams, E. R. Proton Affinity and Zwitterion Stability: New Results from Infrared Spectroscopy and Theory of Cationized Lysine and Analogues in the Gas Phase. *J. Phys. Chem. A* **2009**, *113*, 431−438.

(4) Price, W. D.; Jockusch, R. A.; Williams, E. R. Is Arginine a Zwitterion in the Gas Phase? *J. Am. Chem. Soc.* **1997**, *119*, 11988.

(5) Kong, X. Reinvestigation of the Structure of Protonated Lysine Dimer. *J. Am. Soc. Mass Spectrom.* **2014**, *25*, 422−426.

(6) Alahmadi, Y. J.; Gholami, A.; Fridgen, T. D. The Protonated and Sodiated dimers of Proline Studied by IRMPD Spectroscopy in the N−H and O−H Stretching Region and Computational Methods. *Phys. Chem. Chem. Phys.* **2014**, *16*, 26855−26863.

(7) Wu, R.; McMahon, T. B. Infrared Multiple Photon Dissociation Spectra of Proline and Glycine Proton-Bound Homodimers. Evidence for Zwitterionic Structure. *J. Am. Chem. Soc.* **2007**, *129*, 4864−4865.

(8) Yin, H.; Kong, X. Structure of Protonated Threonine Dimers in the Gas Phase: Salt-Bridged or Charge-Solvated? *J. Am. Soc. Mass Spectrom.* **2015**, *26*, 1455−1461.

(9) Kong, X.; Tsai, I.-A.; Sabu, S.; Han, C.-C.; Lee, Y. T.; Chang, H.-C.; Tu, S.-Y.; Kung, A. H.; Wu, C.-C. Progressive Stabilization of Zwitterionic Structures in [H(Ser)2−8]+ Studied by Infrared Photodissociation Spectroscopy. *Angew. Chem.* **2006**, *118*, 4236−4240.

(10) Seo, J.; Hoffmann, W.; Malerz, S.; Warnke, S.; Bowers, M. T.; Pagel, K.; von Helden, G. Side-chain Effects on the Structures of Protonated Amino Acid Dimers: A Gas-phase Infrared Spectroscopy Study. *Int. J. Mass Spectrom.* **2018**, *429*, 115−120 Terry B. McMahon 70th Birthday Special Issue: Mass Spectrometry and its Application to the Physical Chemistry of Gaseous Ions. *Int. J. Mass Spectrom.*Fridgen, T. D., Bohme, D. K., Eds.; **2018**, 1−226.

(11) Klyne, J.; Bouchet, A.; Ishiuchi, S.-i.; Fujii, M.; Schneider, M.; Baldauf, C.; Dopfer, O. Probing Chirality Recognition of Protonated Glutamic Acid Dimers by Gas-phase Vibrational Spectroscopy and First-principles Simulations. *Phys. Chem. Chem. Phys.* **2018**, *20*, 28452−28464.

(12) Price, W. D.; Schnier, P. D.; Williams, E. R. Binding Energies of the Proton-Bound Amino Acid Dimers Gly⊙Gly, Ala⊙Ala, Gly⊙Ala, and Lys⊙Lys Measured by Blackbody Infrared Radiative Dissociation. *J. Phys. Chem. B* **1997**, *101*, 664−673.

(13) Jockusch, R. A.; Lemoff, A. S.; Williams, E. R. Hydration of Valine- Cation Complexes in the Gas Phase: On the Number of Water Molecules Necessary to Form a Zwitterion. *J. Phys. Chem. A* **2001**, *105*, 10929−10942.

(14) Lemoff, A. S.; Bush, M. F.; Williams, E. R. Structures of Cationized Proline Analogues: Evidence for the Zwitterionic Form. *J. Phys. Chem. A* **2005**, *109*, 1903−1910.
(15) Xu, S.; Nilles, J. M.; Bowen, K. H., Jr Zwitterion Formation in Hydrated Amino Acid, Dipole Bound Anions: How Many Water Molecules are Required? *J. Chem. Phys.* **2003**, *119*, 10696−10701.
(16) Oh, H.; Breuker, K.; Sze, S. K.; Ge, Y.; Carpenter, B. K.; McLafferty, F. W. Secondary and Tertiary Structures of Gaseous Protein Ions Characterized by Electron Eapture Dissociation Mass Spectrometry and Photofragment Spectroscopy. *Proc. Natl. Acad. Sci. U. S. A.* **2002**, *99*, 15863−15868.
(17) Oh, H.-B.; Lin, C.; Hwang, H. Y.; Zhai, H.; Breuker, K.; Zabrouskov, V.; Carpenter, B. K.; McLafferty, F. W. Infrared Photodissociation Spectroscopy of Electrosprayed Ions in a Fourier Transform Mass Spectrometer. *J. Am. Chem. Soc.* **2005**, *127*, 4076−4083.
(18) Rodgers, M.; Armentrout, P.; Oomens, J.; Steill, J. Infrared Multiphoton Dissociation Spectroscopy of Cationized Threonine: Effects of Alkali-metal Cation Size on Gas-phase Conformation. *J. Phys. Chem. A* **2008**, *112*, 2258−2267.
(19) Dunbar, R. C.; Steill, J. D.; Oomens, J. Cationized Phenylalanine Conformations Characterized by IRMPD and Computation for Singly and Doubly Charged Ions. *Phys. Chem. Chem. Phys.* **2010**, *12*, 13383−13393.
(20) Kong, X.; Tsai, I.-A.; Sabu, S.; Han, C.-C.; Lee, Y. T.; Chang, H.-C.; Tu, S.-Y.; Kung, A.; Wu, C.-C. Progressive Stabilization of Zwitterionic Structures in [H (Ser) 2−8]+ Studied by Infrared Photodissociation Spectroscopy. *Angew. Chem., Int. Ed.* **2006**, *45*, 4130−4134.
(21) Kong, X.; Lin, C.; Infusini, G.; Oh, H.-B.; Jiang, H.; Breuker, K.; Wu, C.-C.; Charkin, O. P.; Chang, H.-C.; McLafferty, F. W. Numerous Isomers of Serine Octamer Ions Characterized by Infrared Photodissociation Spectroscopy. *ChemPhysChem* **2009**, *10*, 2603−2606.
(22) Liao, G.; Yang, Y.; Kong, X. Chirality Effects on Proline-substituted Serine Octamers Revealed by Infrared Photodissociation Spectroscopy. *Phys. Chem. Chem. Phys.* **2014**, *16*, 1554−1558.
(23) Wu, R.; McMahon, T. B. Stabilization of the Zwitterionic Structure of Proline by an Alkylammonium Ion in the Gas Phase. *Angew. Chem., Int. Ed.* **2007**, *46*, 3668−3671.
(24) Wu, R.; Marta, R. A.; Martens, J. K.; Eldridge, K. R.; McMahon, T. B. Experimental and Theoretical Investigation of the Proton-bound Dimer of Lysine. *J. Am. Soc. Mass Spectrom.* **2011**, *22*, 1651.
(25) Bush, M. F.; Oomens, J.; Saykally, R. J.; Williams, E. R. Effects of Alkaline Earth Metal Ion Complexation on Amino Acid Zwitterion Stability: Results from Infrared Action Spectroscopy. *J. Am. Chem. Soc.* **2008**, *130*, 6463−6471.
(26) Bush, M. F.; Oomens, J.; Williams, E. R. Proton Affinity and Zwitterion Stability: New Results from Infrared Spectroscopy and Theory of Cationized Lysine and Analogues in the Gas Phase. *J. Phys. Chem. A* **2009**, *113*, 431−438.
(27) O'Brien, J. T.; Prell, J. S.; Steill, J. D.; Oomens, J.; Williams, E. R. Interactions of Mono-and Divalent Metal Ions with Aspartic and Glutamic Acid Investigated with IR Photodissociation Spectroscopy and Theory. *J. Phys. Chem. A* **2008**, *112*, 10823−10830.
(28) Prell, J. S.; Chang, T. M.; Biles, J. A.; Berden, G.; Oomens, J.; Williams, E. R. Isomer Population Analysis of Gaseous Ions from Infrared Multiple Photon Dissociation Kinetics. *J. Phys. Chem. A* **2011**, *115*, 2745−2751.
(29) Polfer, N. C.; Oomens, J. Vibrational Spectroscopy of Bare and Solvated Ionic Complexes of Biological Relevance. *Mass Spectrom. Rev.* **2009**, *28*, 468−494.
(30) Bleiholder, C.; Suhai, S.; Paizs, B. Revising the Proton Affinity Scale of the Naturally Occurring α-amino Acids. *J. Am. Soc. Mass Spectrom.* **2006**, *17*, 1275−1281.
(31) Francuski, B. M.; Novaković, S. B.; Bogdanović, G. A. Electronic Features and Hydrogen Bonding Capacity of the Sulfur Acceptor in Thioureido-based Compounds. Experimental Charge Density Study of 4-methyl-3-thiosemicarbazide. *CrystEngComm* **2011**, *13*, 3580−3591.
(32) Biswal, H. S.; Bhattacharyya, S.; Bhattacherjee, A.; Wategaonkar, S. Nature and Strength of Sulfur-centred Hydrogen Bonds: Laser Spectroscopic Investigations in the Gas Phase and Quantum-chemical Calculations. *Int. Rev. Phys. Chem.* **2015**, *34*, 99−160.
(33) Aradi, B.; Hourahine, B.; Frauenheim, T. DFTB+, a Sparse Matrix-based Implementation of the DFTB Method. *J. Phys. Chem. A* **2007**, *111*, 5678−5684.
(34) Density Functional Based Tight Binding (and more). https://www.dftbplus.org/, Accessed 2019-02-12.
(35) Yatsyna, V.; Bakker, D. J.; Feifel, R.; Rijs, A. M.; Zhaunerchyk, V. Aminophenol Isomers Unraveled by Conformer-specific far-IR Action Spectroscopy. *Phys. Chem. Chem. Phys.* **2016**, *18*, 6275−6283.
(36) Frisch, M. J.; Trucks, G. W.; Schlegel, H. B.; Scuseria, G. E.; Robb, M. A.; Cheeseman, J. R.; Scalmani, G.; Barone, V.; Petersson, G. A.; Nakatsuji, H., et al. *Gaussian 16*, Revision C.01; Gaussian Inc.: Wallingford, CT, 2016.
(37) Halls, M. D.; Velkovski, J.; Schlegel, H. B. Harmonic Frequency Scaling Factors for Hartree-Fock, S-VWN, B-LYP, B3-LYP, B3-PW91 and MP2 with the Sadlej pVTZ Electric Property Basis Set. *Theor. Chem. Acc.* **2001**, *105*, 413−421.
(38) Johnson, E. R.; Keinan, S.; Mori-Sánchez, P.; Contreras-García, J.; Cohen, A. J.; Yang, W. Revealing Noncovalent Interactions. *J. Am. Chem. Soc.* **2010**, *132*, 6498−6506.
(39) Contreras-García, J.; Yang, W.; Johnson, E. R. Analysis of Hydrogen-bond Interaction Potentials from the Electron Density: Integration of Noncovalent Interaction Regions. *J. Phys. Chem. A* **2011**, *115*, 12983−12990.
(40) Oh, H.-B.; Lin, C.; Hwang, H. Y.; Zhai, H.; Breuker, K.; Zabrouskov, V.; Carpenter, B. K.; McLafferty, F. W. Infrared Photodissociation Spectroscopy of Electrosprayed Ions in a Fourier Transform Mass Spectrometer. *J. Am. Chem. Soc.* **2005**, *127*, 4076−4083.
(41) Adesokan, A. A.; Gerber, R. Anharmonic Vibrational Spectroscopy Calculations for Proton-bound Amino Acid Dimers. *J. Phys. Chem. A* **2009**, *113*, 1905−1912.
(42) Almasian, M.; Grzetic, J.; van Maurik, J.; Steill, J. D.; Berden, G.; Ingemann, S.; Buma, W. J.; Oomens, J. Non-equilibrium Isomer Distribution of the Gas-phase Photoactive Yellow Protein Chromophore. *J. Phys. Chem. Lett.* **2012**, *3*, 2259−2263.
(43) Oomens, J.; Moore, D. T.; Meijer, G.; von Helden, G. Infrared Multiple Photon Dynamics and Spectroscopy of Cationic PABA and its Dehydroxylated Fragment Ion. *Phys. Chem. Chem. Phys.* **2004**, *6*, 710−718.
(44) Maître, P.; Le Caër, S.; Simon, A.; Jones, W.; Lemaire, J.; Mestdagh, H.; Heninger, M.; Mauclaire, G.; Boissel, P.; Prazeres, R. Ultrasensitive Spectroscopy of Ionic Reactive Intermediates in the Gas Phase Performed with the First Coupling of an IR FEL with an FTICR-MS. *Nucl. Instrum. Methods Phys. Res., Sect. A* **2003**, *507*, 541−546.
(45) Bouchoux, G. From the Mobile Proton to Wandering Hydride Ion: Mechanistic Aspects of Gas-phase Ion Chemistry. *J. Mass Spectrom.* **2013**, *48*, 505−518.
(46) Poline, M.; Rebrov, O.; Larsson, M.; Zhaunerchyk, V. Theoretical Studies of Infrared Signatures of Proton-bound Amino Acid Dimers with Homochiral and Heterochiral Moieties. *Chirality* **2020**, *32*, 359−369.
(47) Headrick, J. M.; Diken, E. G.; Walters, R. S.; Hammer, N. I.; Christie, R. A.; Cui, J.; Myshakin, E. M.; Duncan, M. A.; Johnson, M. A.; Jordan, K. D. Spectral Signatures of Hydrated Proton Vibrations in Water Clusters. *Science* **2005**, *308*, 1765−1769.

https://dx.doi.org/10.1021/acs.jpca.9b11811
J. Phys. Chem. A 2020, 124, 2408−2415